http://ansinet.com/itj

ITJ

ISSN 1812-5638

INFORMATION TECHNOLOGY JOURNAL

ANSInet
Asian Network for Scientific Information
308 Lasani Town, Sargodha Road, Faisalabad - Pakistan

Information Technology Journal 10 (8): 1498-1507, 2011
ISSN 1812-5638 / DOI: 10.3923/itj.2011.1498.1507

Design and Performance Analysis of Transmitted Signal Waveforms with Spread Spectrum Technology for Netted Radar System

Lianqing Fu, Shizhong Yang, Tao Wang and Yaning Ma
Center of Communication and Tracking Telemetering Command,
Chongqing University, Chongqing, 400044, China

Abstract: In this study, the important function of netted radar system is discussed and its serious problem that mutual interference between transmitted signals, when it works in practice. In order to reduce the influence of mutual interference between signals, a novel netted radar system is designed. Transmitted signal of each station is assigned a unique Pseudo Noise (PN) code and all the PN codes from different stations are orthogonal. Because of the good autocorrelation and cross-correlation properties, mutual interference becomes weaker and signals from different stations could be separated by the preassigned PN codes and several radar stations can be active simultaneously. At the same time, the spectrum of the emission signal is spreaded, the Peak-to-mean Envelope Power Ratio (PMEPR) and the intercepted probability of the signals descend therefore. Simulation results show the good performance of the proposed approach and real radar system's detect result confirms the proposal.

Key words: Anti-stealth technology, spread spectrum, netted radar, PN code, radar, ambiguity function

INTRODUCTION

Stealth Aircrafts and Antiradar Missiles (ARMS) have become serious growing threats to military radars. In modern wars, stealth aircrafts and antiradar missiles are deathful weapons and anti-stealth technology is the most important factor for improving anti-air capability. So the capability of the radar must be extend to cover anti-stealth and anti-ARM, especially in weaker countries. Plenty of research has been done in anti-stealth and anti-ARM technology. According to anti-stealth theory, researchers have designed passive radar, multistatic radar, low frequency radar, ultrawide band radar, spread spectrum radar, netted radars and so on (Rao and Mahulikar, 2002; Li, 1995; Mei and Yu, 2010; Yu *et al*., 2007). Multistatic radar and netted radars are promising technologies for future radar systems. Signals transmitted by several synchronous radar stations can be processed coherently to increase the SNR at the receiver, thus the detection range broadens and the detection performances improve. It means that each station can transmit a lower power which makes them less expensive to build and less detectable by enemy radars (Men *et al*., 2009; Lotfi *et al*., 2010; Abdullah *et al*., 2009).

A lot of research indicates that multi-static and netted radars are able to implement anti-stealth. But the ability is restrained for mutual interference between the signals emitted from different stations (Yin *et al*., 2011; Reddy *et al*., 2008). At the same time, when it comes to stealth aircrafts, receivers usually need to know which station the received signal comes from. The idea of time division multiplexing is used in netted radar system. Different radar transmitters do not illuminate same air space at the same time. Mutual interference is restrained but detectivity of radars is not perfect (Johnsen *et al*., 2004). Orthogonal multi-carrier phased coded signal is designed to restrict the mutual interference which will make the system complex to achieve it (Paichard, 2009). Orthogonal Frequency Division Multiplexing (OFDM) signal is utilized in multi-static and netted radars, however the synchronization technique is difficult and the received data is not precise (Paichard, 2010). Multi-band frequency signals can restrict the mutual interference and the transmitters are known but antenna bandwidth of the receivers must be very wide and the data fusion is very inconvenient (Han and Nguyen, 2007).

In this study, a new netted radar system is designed and it combines the advantages of netted radar and spread spectrum technology. In the proposed radar system, several radars with different PN codes are located at different places and they are activated simultaneously, the good auto-correlation and cross-correlation properties of PN codes limit the mutual interference of signals. As a result, the anti-stealth ability of netted radars is developed. Moreover, each radar station is assigned a different PN code and the emission signals will be

Correspondimg Author: Lianqing Fu, Center of Communication and Tracking Telemetering Command, Chongqing University, Chongqing, 400044, China

distinguished by Digital Matched Filters (DMF) at the receivers. Several radars are located at different places and they are active simultaneously, so it is easy to optimize the coverage area. Meanwhile, radars in net transmit signals at the same time and therefore, the received signal power will be augmented, leading to an increase in overall SNR. Deal to the spread spectrum technology, the PMEPR of the emission signal descends, the intercepted probability of the signals drops and the SNR increases at the receivers.

THE ANTI-STEALTH THEORY OF NETTED RADAR

The stealth theory of aircrafts: In recent years, great progress has taken place in stealth technology of aircrafts. F117 and F22 are the prominent representative of stealth aircrafts. On the whole, the theories of stealth technology are in essence the same and they are shown as follows (Li, 1995). The most important two measures are external shape technique of decreasing RCS and adding surface wave-absorbing coating. Apart from that, wave-absorbing materials are used as structural materials of aircraft and the structural compound materials include wave-absorbing materials and wave-penetrating nonmetal materials. And impedance load technique is another important one. Since these measures are adopted, the aircrafts are difficult to detect and the detection range is narrowed down seriously.

The anti-stealth theory of netted radar: Although, a big advance has been made in stealth technology recently, it is found that the stealth aircrafts are not completely invisible. ‘Frequency window’ and ‘space window’ are left for us to find them. Engineers have done much research in how to counter stealth technology. Multistatic and netted radars are proved the most valuable way to anti-stealth. External shape stealth technique of decreasing RCS is resolved well with netted radars system. For that the design of external shape achieves the purpose of stealth by means of changing backward scatter direction from arrival direction and there is little backward scatter, especially in nose cone direction. However, emitting station and receiving station are located at different places, this makes some radars can observe air vehicle from side, back or bottom. A preliminary research into netted radar for anti-stealth is done and it shows us that networks of radar sensors can offer a counter to stealth technology through receiving backward scatter from different directions (Jinlei *et al*., 1998). The illustrative diagram is shown in Fig. 1.

In Fig. 1, receiver 1 may cannot receive backward scatter of transmiter1 because of the aircraft’s external shape design but it can receive signal from transmiter 2 and receiver 2 is the same. Another advantage of netted radar system is that one single large radar can be splitted into several small radars (Baker and Hume, 2003). Each of the small radars are monostatic and independent. The launching power of each radar is lower than the large one which makes radars less expensive to build for us and more difficult to discover by enemy radars. The detection range of the two radars is shown in Fig. 2.

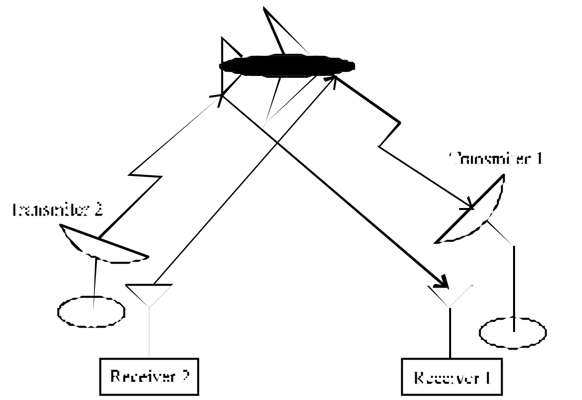

Fig. 1: The fundamental principle of netted radars

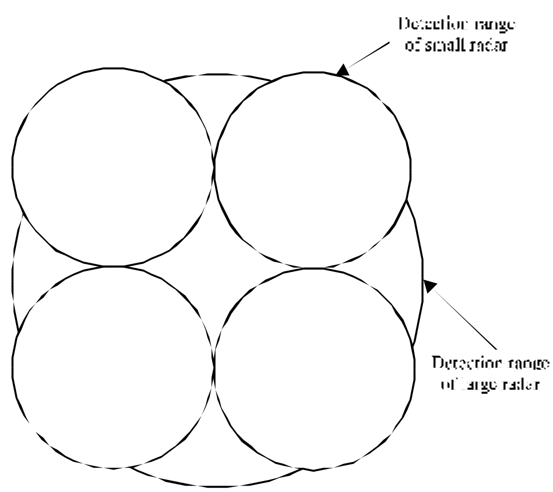

Fig. 2: Detection ranges of four small radars and one large radar

Moreover, the netted radar has lots of other advantages. Firstly, it is easy to optimize the coverage area and the deployment is flexible. Secondly, due to the additional use of radar transmitters, the received signal power will be augmented, leading to an increase in overall SNR. Thirdly, the survivability and reliability of netted radars are improved significantly. The loss of one or even several stations may not be fatal, because there are still some other stations working well (Teng *et al.*, 2007; Paichard *et al.*, 2009).

DESIGN OF NEW RADAR SYSTEM

Design of the system: Here, a novel netted radar system with spread spectrum technology is designed. This system combines all advantages of traditional netted radars system and it can also eliminate the influence of signals mutual interference. Signals from different transmitters can be distinguished too.

The system diagram of new netted radars system is shown in Fig. 3. In this system, some radar stations are located on land and some are in the sky. They are activated simultaneously. Hostile aircrafts in this system are irradiated from many different directions, so some radar stations can receive scatter from side, back, tail or bottom. External shape stealth technique disables when aircrafts are under this situation. In addition, one important characteristic of the system is the emission signals. Every station has a fixed PN code and the signal is coded with it before launching. At receiving terminal, these signals can be separated and synthesized well because of the good auto-correlation and cross-correlation properties of PN codes. The theory of spread spectrum netted radars is shown as follows. At the transmitting terminals, the composition of each station is the same except the PN code. Different PN codes are assigned to different stations.

The transmitting schematic diagram of one station is shown in Fig. 4 where, d (t) is multiplied by c_n (t) and the result is modulated up to emission frequency. S_n (t), n = 1, 2 is transmitted signal shown as follows:

$$s_n(t) = d(t) \times \cos(\omega_0 t) \quad (1)$$

Several stations are activated at the same time, so s_n (t) is mixed with other emission signals, Gaussian white noise and interference signals in the propagating process. When ignoring the influence of the multiplicative interference signal, r (t) is got:

$$r(t) = Ks(t-\tau) + w(t) + J(t)$$
$$s(t) = d(t) \times [c_1(t) + c_2(t) + \ldots + c_n(t)] \times \cos \quad (2)$$

where, w (t) is Gaussian white noise, J (t) is interference signal, K is a constant, τ is transmission delay c_1 (t) c_2 (t) ... c_n (t) are PN codes from different stations. As a result, the components of receiver are shown in Fig. 5.

In Fig. 5, DMF is the abbreviation of digital matched filter. At the receiving terminal, r (t) is processed by high-frequency amplifier, mixing and N digital matched filters. If the PN codes of transmitter and receiver are synchronous accurately, then d_i (t) is achieved:

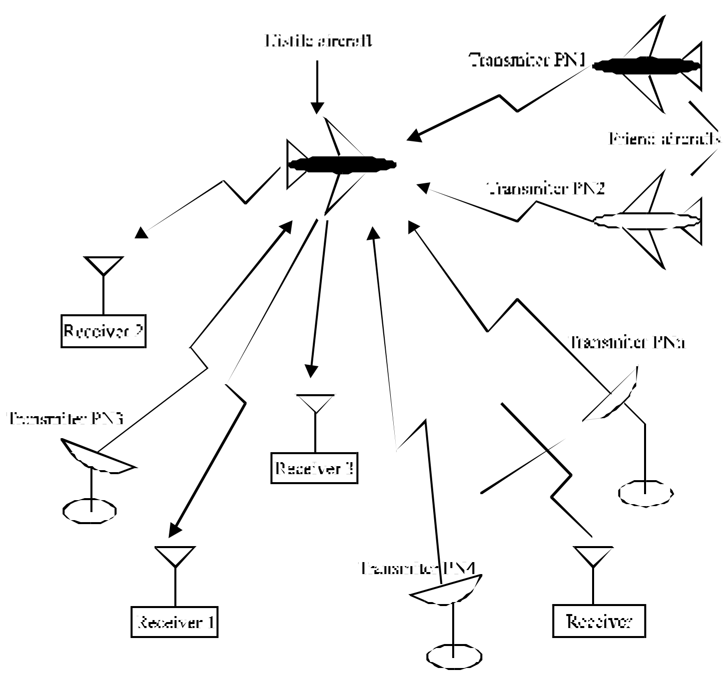

Fig. 3: Block diagram of new netted radars system

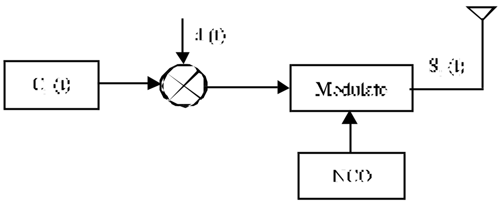

Fig. 4: Transmitting schematic diagram

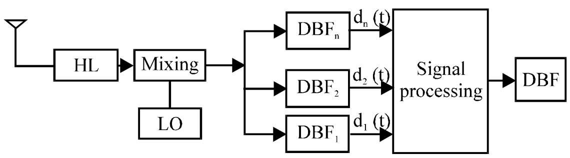

Fig. 5: Components of receiver

$$d_i\,(t) = Kd\,(t)\times[c_1\,(t\text{-}\tau)_1 + c_2\,(t\text{-}\tau) + ... + c_n\,(t\text{-}\tau)]\times c_1\,(t\text{-}\tau)\times\cos\,(\omega_0\,t\text{-}\tau) + w\,(t)\times c_1\,(t\text{-}\tau) + J\,(t)\times c_1\,(t\text{-}\tau),\ I = 1, 21\ ...,, n \quad (3)$$

Since $c^2\,(t\text{-}\tau) \equiv 1$ and the PN codes are orthogonal to each other:

$$d_i\,(t) = Kd\,(t)\times\cos\,(\omega_0\,t\text{-}\tau) + w\,(t)\times c_1\,(t\text{-}\tau) + J\,(t)\times c_1\,(t\text{-}\tau),\ I = 1, 2, ..., n \quad (4)$$

In Eq. 4, Kd $(t)\times\cos\,(\omega_0\,t\text{-}\tau)$ is wanted signal, w $(t)\times c_1\,(t\text{-}\tau)$ and J $(t)\times c_1\,(t\text{-}\tau)$ are interference signals and their spectral density is much lower than before. Receiver can synthesize and process these signals in order to get original signal after demodulation. The SNR of receiver increases therefore. Because of the good autocorrelation and cross-correlation properties of PN codes the mutual interference of signals in netted radars is eliminated and the emission signals can be distinguished by digital matched filters at the receivers.

Key technologies in the designed system: There are lots of difficulties in designing a netted radars system, such as the radars' rational layout, the global ambiguity function in the signal processing system and so on. However, the main difficulty of designing such a system is the fast acquisition of PN codes. The stealth aircrafts are very fast when they are on duty, so the fast acquisition of PN codes is requisite and Doppler frequency shift must not be disregarded either (Gross and Chen, 2005; Horvath *et al.*, 2009). For these reasons, a new acquisition system is designed. The components of acquisition system are shown in Fig. 6.

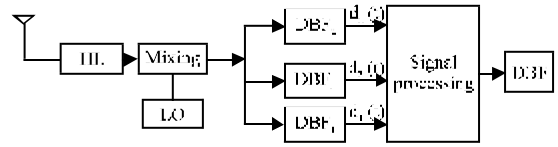

Fig. 6: Components of acquisition system

In this system, Intermediate Frequency (IF) signal is mixed with the Center Frequency signal of Costas Loop. Then the frequency offset is calculated by FFT. Because sometimes the Doppler frequency shift is very large, coarse estimate of frequency offset is used to adjust the initial frequency control word of Costas Loop. And the frequency difference between IF signal and signal of Costas Loop is small enough. Then the fast acquisition is easy for Costas Loop and DMF.

AMBIGUITY FUNCTION OF TRANSMITTED SIGNALS

Here, radar ambiguity function and the performance of signals designed with spread spectrum technology in netted radar system is researched. The radar ambiguity function represents the output of the matched filter and it describes the interference caused by range and/or Doppler of a target when compared to a reference target of equal RCS (Mahafza, 2000; Levanon and Mozeson, 2004). Usually, ambiguity function can be used to analyze the resolution of radar signals and it is first introduced by Woodward. Radar ambiguity function is defined as:

$$|\chi(\tau, f_d)| = \left|\int_{-\infty}^{+\infty} s(t)s^*(t-\tau)\exp(j2\pi f_d t)dt\right| \quad (5)$$

where, τ is time delay and f_d is doppler frequency shift. The ambiguity function evaluated at $(\tau, f_d) = (0, 0)$ is equal to the matched filter output that is matched perfectly to the signal reflected from the target of interest. The radar ambiguity function is normally used by radar designers as a means of studying different waveforms. It can provide insight about how different radar waveforms may be suitable for the various radar applications. In order to illustrate good performance of signals designed in this study, single pulse ambiguity function, signal pulse with short PN code and signal pulse with long PN code ambiguity function are shown.

Traditional single pulse ambiguity function: Single rectangular pulse is defined by:

$$s(t) = \frac{1}{\sqrt{\tau'}} \mathrm{Rect}(\frac{t}{\tau'}) \quad (6)$$

From Eq. 5:

$$|\chi(\tau, f_d)| = \left| \int_{-\infty}^{+\infty} s(t) s^*(t-\tau) \exp(j2\pi f_d t) dt \right| \quad (7)$$

Substituting Eq. 6 into 7, it can be integrated and got:

$$|\chi(\tau, f_d)| = \left| (1 - \frac{|\tau|}{\tau'}) \frac{\sin(\pi f_d(\tau' - |\tau|))}{\pi f_d(\tau' - |\tau|)} \right| |\tau| \le \tau' \quad (8)$$

In the simulation, it is assumed that pulse width τ is 0.7 sec and τ' is 0.7 sec. Figure 7 (a-b) shows 3-D and contour plot of single pulse uncertainty and ambiguity functions.

The ambiguity function cut along the time delay axis τ shows time ambiguity and it is obtained by setting $f_d = 0$. Figure 8a shows time delay uncertainty function when doppler frequency f_d is zero. Similarly, the ambiguity function cut along the doppler frequency axis shows velocity ambiguity function and it is obtained by setting $\tau = 0$. Figure 8b shows velocity uncertainty function when time delay is zero.

Ambiguity function of signal pulse with short PN code (Horvath *et al.*, 2009): In this part, ambiguity function of signal pulse with short PN code is shown. Two short PN codes are employed in the simulation and they are C_1 (t) = 1110100 and C_2 (t) = 1100101. The ambiguity function and the cross-ambiguity function shows the good auto-correlation and cross-correlation properties of PN codes. Signal pulse signal with seven bits PN code is defined by:

$$s(t) = \frac{1}{\sqrt{\tau'}} \mathrm{Rect}(\frac{t}{\tau'}) C_1(t) \quad (9)$$

Assuming that rectangular pulse is seven times the width of C_1 (t), so Eq. 9 is equivalent to:

$$s(t) = \frac{1}{\sqrt{\tau'}} \mathrm{Rect}(\frac{t}{\tau'}) \{[u(t+\frac{\tau'}{2}) - u(t+\frac{\tau'}{14})] + [u(t-\frac{\tau'}{14}) - u(t+\frac{\tau'}{14})] + [u(t-\frac{\tau'}{14}) - u(t-\frac{3\tau'}{14})] + [u(t-\frac{\tau'}{2}) - u(t-\frac{3\tau'}{14})]\} \quad (10)$$

From Eq. 5:

$$|\chi(\tau, f_d)| = \left| \int_{-\infty}^{+\infty} s(t) s^*(t-\tau) \exp(j2\pi f_d t) dt \right| \quad (11)$$

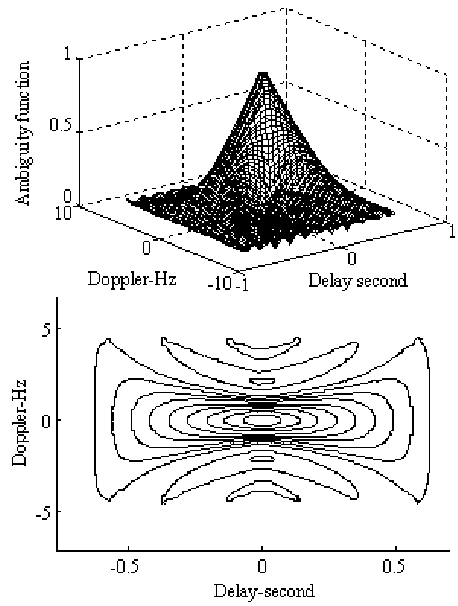

Fig. 7: Single pulse 3-D uncertainty plot Fig. 7b Contour plot corresponding to Fig. 7a

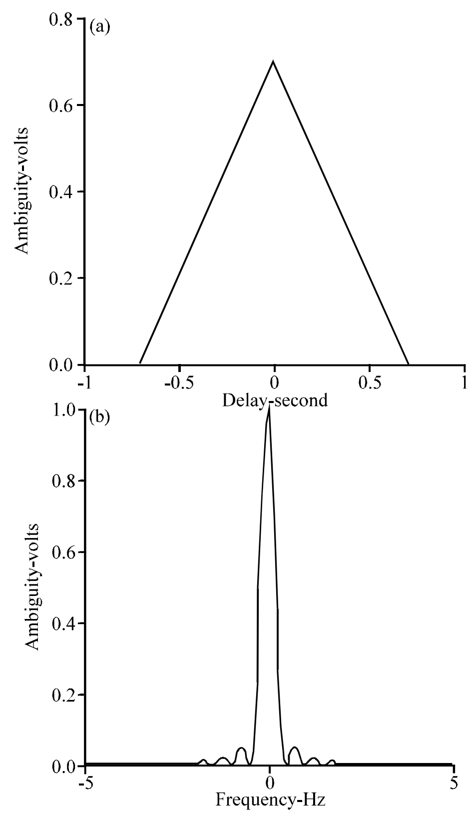

Fig. 8(a-b): (a) Zero Doppler uncertainty function cut along the time delay axis (b) Uncertainty function of a single frequency pulse

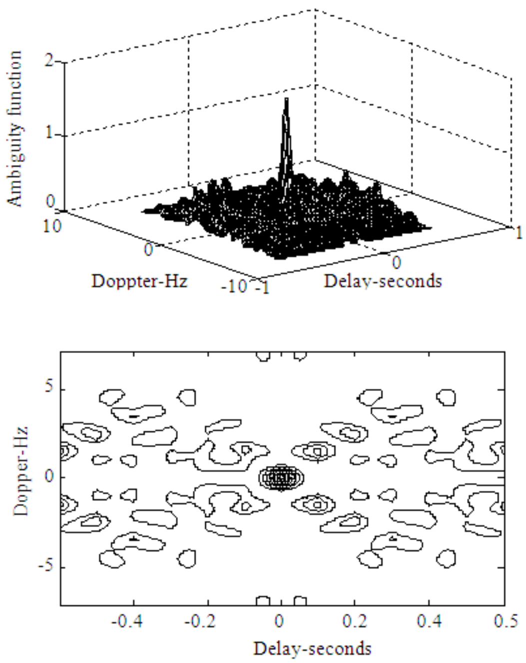

Fig. 9: Single pulse 3-D uncertainty plot Fig. 9b Contour plot corresponding to Fig. 9a

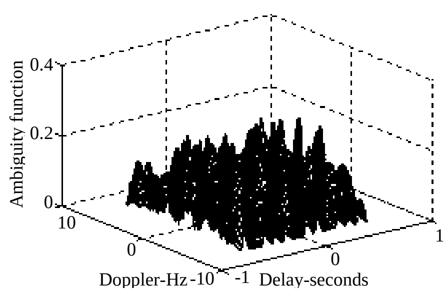

Fig. 10: Cross-ambiguity function of C_1 (t) and C_2 (t)

Substituting Eq. 10 into 11, simulate it in matlab with τ' = 0.7 sec, uncertainty and ambiguity functions is got. Fig. 9 (a-b) shows 3-D and contour plot of seven bits PN codes uncertainty and ambiguity functions.

From Fig. 9a it can be seen that the peak is more sharper than single pulse. Cross-ambiguity function of C_1 (t) and C_2 (t) is also given in Fig. 10. From Fig. 10 it can be seen that cross-ambiguity peaks are low and they could be ignored.

Ambiguity function of signal pulse with long pn code: In practice, the influence of mutual interference between signals could not be reduced sufficiently, when short PN codes are used in netted radar system.

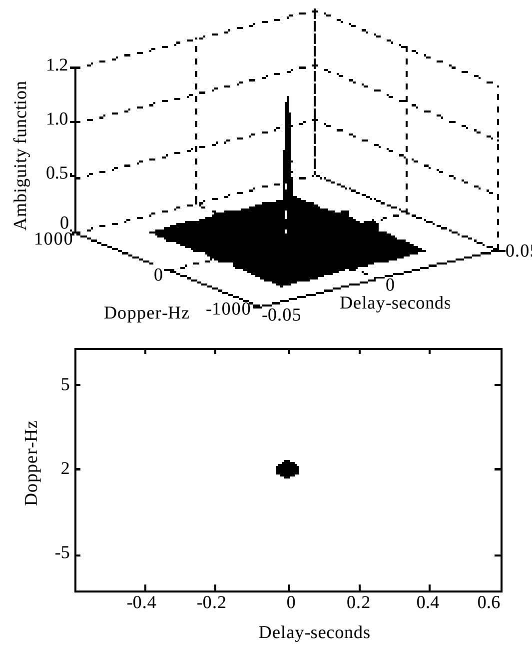

Fig. 11: Single pulse 3-D uncertainty plot Fig. 11b Contour plot corresponding to Fig. 11a

In order to get good performance, long PN codes are employed. The procession is the same as short PN codes' but the performance is perfect. The arithmetic expression of ambiguity function is complicated because of the large amount of stochastic pulse. Figure 11a-b shows 3-D and contour plot of 1023 bits PN codes uncertainty and ambiguity functions.

From Fig. 11a, it can be seen that ambiguity function peak of 1023 bits PN codes is much sharper than seven bits'. In this part, time delay uncertainty function and Doppler frequency uncertainty function is given too. In the simulation, 1023 bits PN code is used and the primitive polynomial coefficients of the sequence are 10000011011 (c_{10}... c_0). Time delay uncertainty function with zero Doppler frequency is shown in Fig. 12.

Setting $\tau = 0$, Doppler frequency uncertainty function is got. When time delay is zero, received signal is the same as a single frequency pulse and its Doppler frequency uncertainty function is shown in Fig. 8b.

Only good autocorrelation property is not enough if receiver wants to separate signals from different radar transmitters and good autocorrelation property is requisite. Long PN codes have not only good autocorrelation property but also good cross-correlation property. Any two PN codes' is weak. Two 1023 bits PN codes with the primitive polynomial coefficients of the sequence 10000011011 (c_0 ... c_{10}) and 11011000001 (c_0 ...c_{10})

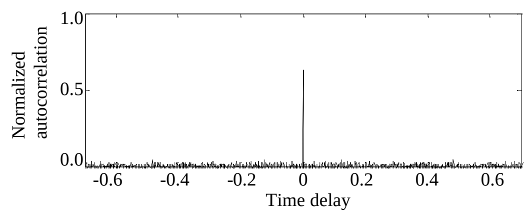

Fig. 12: Normalized range ambiguity function of PN code whose length is 1023 bits

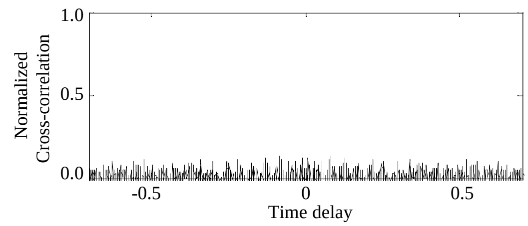

Fig. 13: Normalized cross-correlation function of two PN codes whose length is 1023 bits

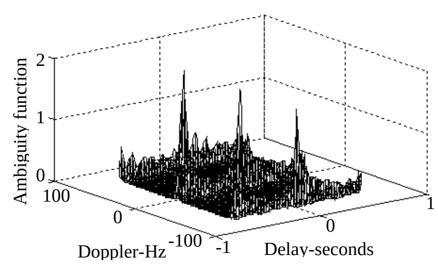

Fig. 14: Ambiguity function of 7 bits PN code with $\tau' = 0.7$ sec

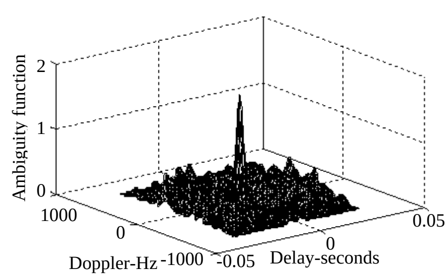

Fig. 15: Ambiguity function of 7 bits PN code with $\tau' = 0.035$ sec

are used. The cross-correlation function of these two PN codes is shown in Fig. 13. It can be concluded from Fig. 11 that cross-correlation property is weak and signals could be separated by DMF perfectly.

Doppler effects analysis of PN codes: PN sequences are well-known to be very sensitive to Doppler shift and that is a strong limitation in a netted context. In this part, Doppler effects of seven bits PN code is shown. With a lot of simulation of PN code, it is found that doppler effect is relevant to the width of PN code and the duration of signal. In other words, the shorter signal is the less influence will be. From Fig. 9 it can be seen that when delay time is 0.7 sec and doppler frequency shift is less than 5Hz, the influence of false peaks could be neglect. But when doppler frequency shift is greater than 50 Hz, the influence of false peaks is serious. Figure 14 shows the ambiguity function of 7 bits PN code when doppler frequency is lager than 50 Hz.

It is quite obvious that doppler frequency shift that could be beared cannot to meet the needs of a real radar detect system. In practice, take metrewave radar for an example, wavelength λ is about a few metres and the velocity of targets must be less than 50 m sec^{-1}. This detect system is useless in practice. If detectors want to raise the radar's detect velocity of target, pulse width must be narrower and bit rate of PN code must be higher. Figure 15 shows ambiguity function of 7 bit PN code when $\tau' = 0.03$ sec and bandwidth of PN code is 1 KHz. In engineering fields, it is easy to implement.

From Fig. 15 it can be seen that when doppler frequency shift is lager than 500Hz false peak still has little effect on detection.

SIMULATION AND EXPERIMENT RESULTS

In this section, a system for separating radar signals from others is designed. In the designed system, radar frequency f_0 is 1030 MHz, the frequency of IF signal is 70 MHz, bandwidth of PN codes is 1 MHz. Assuming that there four radar stations in this system and they are assigned different PN codes whose length are 1023 bits.

Traditional netted radar system without spread spectrum technology: In traditional netted radar system, emission signal from each station is the same. Assuming that the emission signal is d (t):

$$d(t) = m(t) \times \sin(1030000000 \times 2\pi \times t + \Delta\varphi \quad (12)$$

At the receiving terminal, the receiver gets s (t):

$$s(t) = k_1 d(t+\tau_1) + k_2 d(t+\tau_2) + k_3 d(t+\tau_3) + k_4 d(t+\tau_4) w(t) \quad (13)$$

where, k_1 k_2 k_3 and k_4 are reflection coefficients of signals, τ_1 τ_2 τ_3 and τ_4 are delay times of each emission signal and w (t) is noise signal. Waveform of received signal is shown in Fig. 16.

It can be seen from Fig. 16 that signals from each station mix together and mutual interference is heavy. Therefore signals from different stations cannot be separated easily and the data fusion is difficult.

Netted radar system with spread spectrum technology: In this new radar system, four PN codes are assigned to each station and they are orthogonal. The length is 1023 bits and the bandwidth is 1 MHz. c_1 (t), c_2 (t), c_3 (t) and c_4 (t) are the PN codes and their waveforms are shown in Fig. 17.

Assuming that four radar stations are activated simultaneously and four PN codes are assigned to them. The emission signals of the four stations are d_1 (t), d_2 (t), d_3 (t) and d_4 (t):

$$d_i(t) = m(t) \times \sin(300000000 \times 2\pi \times t + \Delta\varphi_i)\; I = 1, 2, 3, 4 \quad (14)$$

where, $\Delta\varphi$ is initial phase of each signal, m (t) is a constant number and its value is 1. At the receiving terminal, received signals are the admixture of d_1 (t) d_2 (t) d_3 (t) and d_4 (t). The receiver gets sec(t):

$$s(t) = k_1 d_1(t+\tau_1) + k_2 d_2(t+\tau_2)\, k_3 d_3(t+\tau_4) + w(t) \quad (15)$$

where, k_1 k_2 k_3 and k_4 are reflection coefficients of signals, τ_1 τ_2 τ_3 and τ_4 are delay times of each emission signal and w (t) is noise signal. Then IF signal is got after down-conversion. Figure 18 shows the waveform of IF signals.

In order to get useful signals for data fusion, carrier synchronization and code synchronization are indispensable. Therefore Costas Loop and DMF are designed in this system. Costas Loop is a key technology in this system and the simulation is shown in Fig. 19.

Where Fig. 19(a) is the input signal and its frequency is 10.5 MHz, Fig. 19(b) is the output signal. It can be seen that the extraction of carrier signal is accurate. DMF is another key technology. Its functions are code synchronization and the separation of different PN codes. The results of code synchronization are shown in Fig. 20.

Figure 20a is input PN code and Fig. 20b is the capture result. It can be seen from Fig. 20 that code synchronization is accurate. IF signal is separated after Costas Loop and DMF. It is clear that which station signal is from with fixed PN codes. The results of separation are shown in Fig. 21.

Each station has a fixed PN code. So the receiver knows that Fig. 21a is from station one, Fig. 21b is from station two, Fig. 21c is from station three and Fig. 21d is

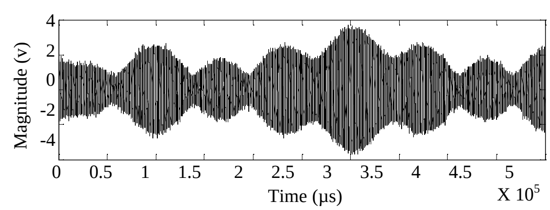

Fig. 16: Waveform of received signal

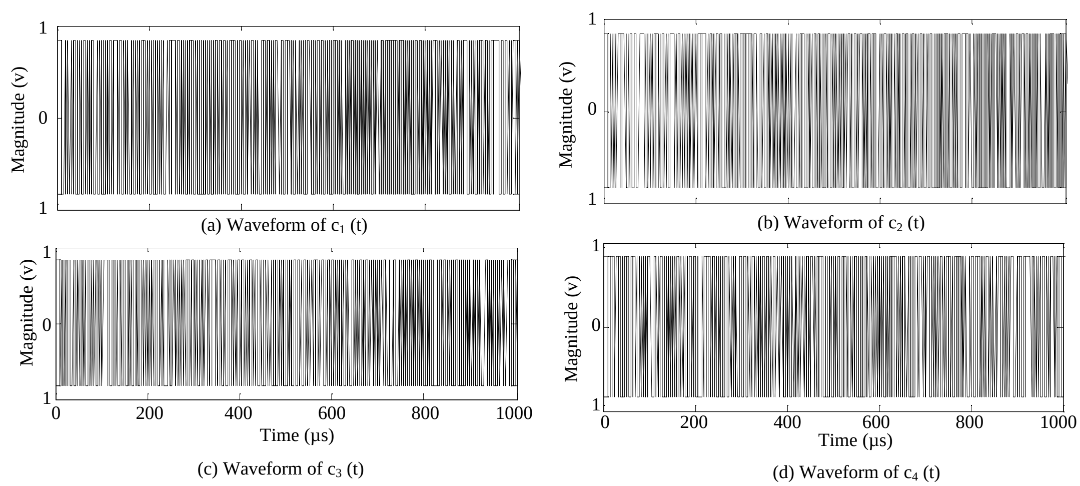

Fig. 17(a-d): Waveforms of PN codes

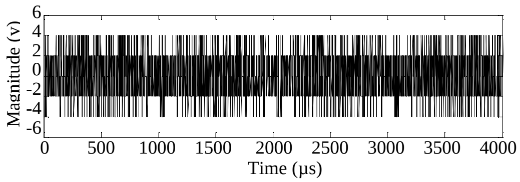

Fig. 18: Waveform of the received signal

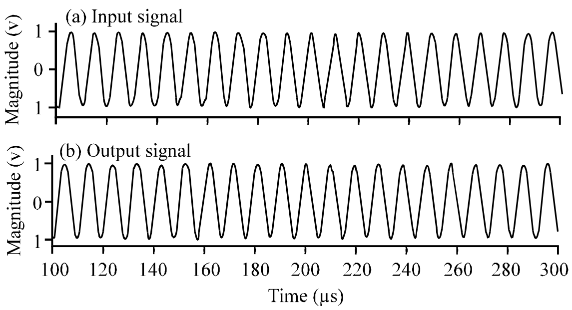

Fig. 19(a-b): Input signal and the synchronization signal

from station four. It can be seen from Fig. 21 that signals from four stations are separated successfully. The mutual interference of signals in the netted radars is eliminated and the receiver knows which station the separated signal comes from. Figure 21 shows baseband signals from each station, with these data receiver can estimate directions that signals come from.

System design implementation of software and hardware: In this part, system implementation of hardware for the proposal in this study is introduced. There are four parts in the system. They are emission source, radio-frequency receiver, baseband signal processing part and display module. The function of this system is detecting aerial attackers and tracking them. Simple-frequency signal of 1030 MHz with PN code could be generated and emitted into the sky. Radio-frequency receiver can receive reflected signal and down-convert 1030MHz to 70MHz. Baseband signal processing part contains three FPGA

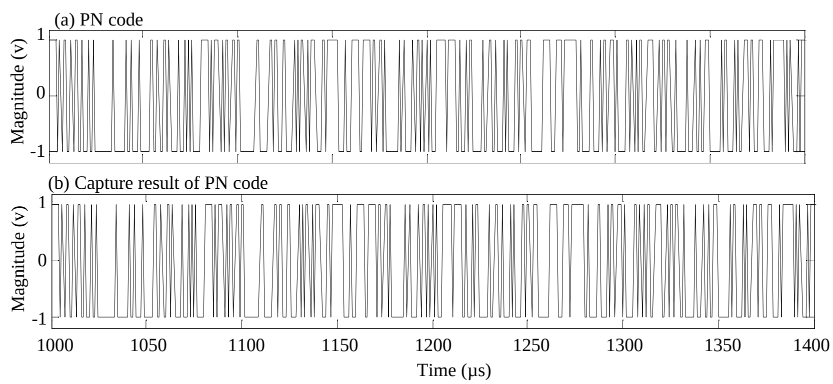

Fig. 20(a-b): PN code and the capture result

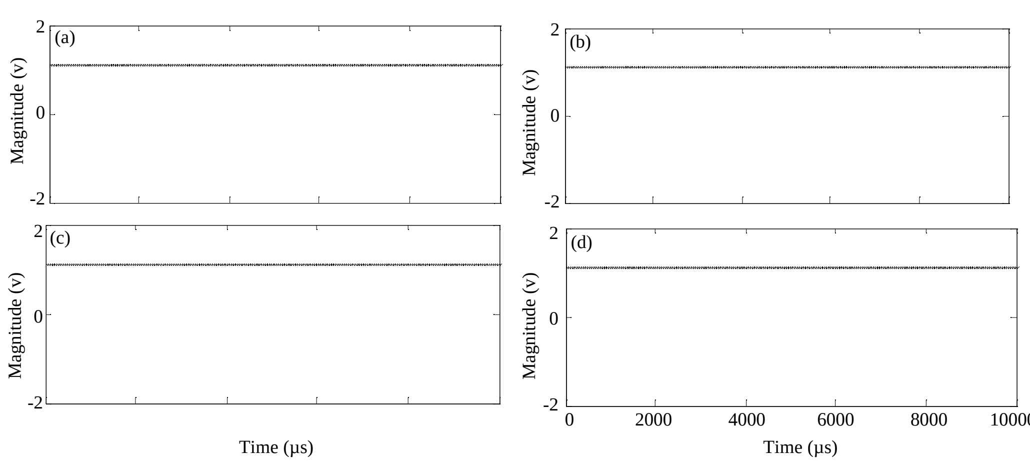

Fig. 21(a-d): The separation of signal from each station chips. The function contains COSTAS LOOP, DMF, DDC and digital beam formation. Display module is a simple monitor.

CONCLUSION

In this study, a novel netted radars system is proposed to decrease the mutual interference. Each radar station is assigned to a fixed PN code. All PN codes have good autocorrelation and cross-correlation properties, so the mutual interference of signals is weakened. Moreover, the signals are distinguished by digital matched filters at the receivers. So the data processing of computers will be easier and the detection will be more accurately. Simulation results show that, mutual interference of signals is suppressed and signals from different stations are separated completely. It is convenient for data fusion by different transmitters with different PN code signals. Hardware implementation system is also shown in this study. We will carry out more research in this field.

Shizhong Yang and Tao Wang developed the concept and all the work is under their direction. Lianqing Fu and Yaning Ma developed the designed experiments. Lianqing Fu and Tao Wang accomplished software and hardware design.

REFERENCES

Abdullah, R.S.A.R., H. Zulhaidi M. Shafri, R. Mardeni, S. Khatun and R. Muniandy, 2009. Evaluation of road pavement density using ground penetrating radar. J. Environ. Sci. Technol., 2: 100-111.

Baker, C.J. and A.L. Hume, 2003. Netted radar sensing. IEEE Aerosp. Electron. Syst. Mag., 18: 3-6.

Gross, F.B. and K. Chen, 2005. Comparison of detectability of traditional pulsed and spread spectrum radar waveforms in classic passive receivers. IEEE Trans. Aerospace Electron. Syst., 41: 746-751.

Han, J. and C. Nguyen, 2007. A multi-band UWB radar for sensing objects. Proceedings of the IEEE Antennas and Propagation Society International Symposium, June 9-15, Honolulu, HI, USA., pp: 4917-4920.

Horvath, M., R. Seller and V. Rosner, 2009. Synthetic aperture radar using spread spectrum modulation. Proceedings of the 19th International Conference Radioelektronika, April 22-23, Bratislava, pp: 149-152.

Jinlei, J., R. Hongbin, G. Fuli and D. Huaisuo, 1998. A preliminary research into the netted radar seekers for anti-stealth aircraft. Proceedings of the 4th International Conferenc Signal Process, Oct. 12-16, Beijing, China, pp: 1566-1569.

Johnsen, T., K.E. Olsen and S. Johnsrud, 2004. Simultaneous use of multiple pseudo random noise codes in multistatic CW radar. Proceedings of the IEEE Radar Conference, April 26-29, Philadelphia, USA., pp: 266-270.

Levanon, N. and E. Mozeson, 2004. Ambiguity Function. In: Radar Signals, Levanon, N. and E. Mozeson (Eds.). Wiley-IEEE, New York, ISBN-13: 9780471473787, pp: 34-44.

Li, N.J., 1995. Radar ECCMs new area: Anti-stealth and anti-ARM. IEEE Trans. Aerospace Electron. Syst., 31: 1120-1127.

Lotfi, A., K. Mezzoug and A. Benyettou, 2010. Rotated kernel neural networks for radar target detection in background noise. J. Applied Sci., 10: 1331-1335.

Mahafza, B.R., 2000. Radar Systems Analysis and Design Using MATLAB. Chapman and Hall/CRC, Ney York.

Mei, H.D. and Z.Q. Yu, 2010. Impulse radio ultra-wide-band through wall imaging radar based on multiple-input multiple-output antenna arrays. Inform. Technol. J., 9: 782-789.

Men, X.S., X.H. Tian and J. Gong, 2009. Study on the capability of near space bistatic radar in detecting stealth targets. Electr. Opt. Contr., 16: 43-46.

Paichard, Y., 2009. Orthogonal multicarrier phased coded signal for netted radar systems. Proceeding of the International Conference Waveform Diversity and Design, Feb. 8-13, Kissimmee, FL, pp: 234-236.

Paichard, Y., 2010. OFDM waveforms for multistatic radars. Proceedings of the IEEE International Radar Conference, May 10-14, Washington DC, USA., pp: 234-236.

Paichard, Y., M. Brooker and M. Inggs, 2009. A signal level simulator for netted radar waveforms evaluation. Proceedings of the International Waveform Diversity and Design Conference, Feb. 8-13, Kissimmee, FL, USA., pp: 278-280.

Rao, G.A. and S.P. Mahulikar, 2002. Integrated review of stealth technology and its role in airpower. Aeronaut. J., 106: 629-641.

Reddy, G.H., Y.V. Reddy and S.N. Reddy, 2008. The effect of β in Kaiser window on the SNR of MST radar signals. Asian J. Scientific Res., 1: 203-212.

Teng, Y., H.D. Griffiths, C.J. Baker and K. Woodbridge, 2007. Netted radar sensitivity and ambiguity. IET Radar Sonar Navig., 1: 479-486.

Yin, Z., W. Yang, Z. Yang, L. Zuo and H. Gao, 2011. A study on radar emitter recognition based on SPDS neural network. Inform. Technol. J., 10: 883-888.

Yu, T., S. Doughty, K. Woodbridge, H. Griffiths and C. Baker, 2007. Netted radar theory and experiments. Proceeding of the Information, Decision and Control, Feb. 12-14, Adelaide, Qld, pp: 23-28.